R. & M. No. 3695

MINISTRY OF DEFENCE (PROCUREMENT EXECUTIVE)

AERONAUTICAL RESEARCH COUNCIL
REPORTS AND MEMORANDA

The Vortex Drag of a Swept Wing with Part-Span Flaps

By H. C. GARNER
Aerodynamics Division, N.P.L.

LONDON: HER MAJESTY'S STATIONERY OFFICE
1972
PRICE 70p NET

The Vortex Drag of a Swept Wing with Part-Span Flaps

By H. C. GARNER

Aerodynamics Division, N.P.L.†

Reports and Memoranda No. 3695*
September, 1970

Summary.

The vortex drag of a lifting surface depends only on its spanwise loading and is usually calculated therefrom. Deflection of a part-span flap gives a theoretical spanwise loading that can only be obtained by numerical approximation in non-analytical form. Subsequent evaluation of vortex drag therefore lacks precision, and two such direct methods are compared. A third method, on the reverse-flow principle, is introduced to determine vortex drag separately from the spanwise loading. For a particular wing-flap combination, the three methods are consistent within $\pm 1\frac{1}{2}$ per cent; this is more than adequate, and in the present state of knowledge no better accuracy is likely to be achieved. Although the third method is rather cumbersome, it provides a ready means of studying the influence of flap span and chord on vortex drag.

LIST OF CONTENTS

† Now Aerodynamics Department, R.A.E., Farnborough.

* Replaces A.R.C. Report 32 395.

1. *Introduction.*

Vortex drag is an elusive quantity to determine by experimental means. Although it is often the major part of the lift-dependent drag, other contributions make it difficult to isolate the vortex drag. In practice, the quantity may well be determined theoretically, and there is some demand for data sheets. For wings alone, the problems are usually manageable. There is, for example, a data sheet issued by the Royal Aeronautical Society[1] (1965) for uncambered and untwisted wings with straight leading and trailing edges in subsonic flow. The vortex drag factor

$$K=1+\delta=\pi A\, C_{Dv}/C_L{}^2 \tag{1}$$

is given for arbitrary aspect ratio A, taper ratio and leading-edge sweepback; accuracy better than 5 per cent is claimed at subcritical Mach numbers.

In Ref. 2 (1968), the author has suggested a simple approximate relationship

$$K=1+\frac{75\pi^2}{16}\left(\bar{\eta}-\frac{4}{3\pi}\right)^2 \tag{2}$$

between the vortex drag factor and the spanwise centre of pressure

$$\bar{\eta}=\frac{2A}{C_L}\int_0^1 \gamma\,\eta\,d\eta\,, \tag{3}$$

where in terms of wing semi-span s, local chord c and local lift coefficient C_{LL} at the section $y=\eta s$

$$\gamma=\tfrac{1}{4}c\,C_{LL}/s\,. \tag{4}$$

The accuracy of equation (2) has recently been checked in Ref. 3, and the formula should serve within ± 2 per cent for all the 64 planforms considered there. It should also suffice for wings with simple distributions of camber and twist. In cases of complicated, but continuous, camber or twist the evaluation of vortex drag follows straightforwardly from a knowledge of the spanwise loading (Section 2). A more difficult theoretical problem is posed by peculiar planforms with severe cranks or cut-outs or chord extensions. Moreover, the wing-body combination cannot yet be treated with any confidence.

Another case that needs careful consideration is that of a wing with deflected part-span trailing-edge flap, which forms the subject of the present investigation. In so far as linearized theory can model the aerodynamic loading in the presence of chordwise and spanwise gaps and strong pressure gradients, the spanwise distribution of lift defines the vortex drag. Analytical solutions are only available in special limiting cases, and one can be faced with markedly different numerical approximations to the spanwise loading dependent on the choice of method. There are proposals for data sheets to give the vortex drag on wings with a combination of flap deflection and angle of attack. As a guide to accuracy, a definitive value of K will be sought for the particular configuration in Fig. 1 with symmetrically deflected outboard flaps and zero angle of attack. Outboard flaps are chosen to minimize any uncertainty due to the central kink of the untapered swept wing. The planform ($A=4$, $\Lambda=45$ degrees) in incompressible flow has already been the subject of theoretical study in Ref. 4 (Garner and Lehrian, 1969). The solution for spanwise loading $\gamma(\eta)$ in Table 1 is taken from Table 15b of Ref. 4 corresponding to flap chord $0{\cdot}25c$, flap span $0{\cdot}45s<|y|<s$ ($\eta_a=0{\cdot}45$) and a nominal flap setting of 1 radian in a vertical streamwise plane.

It would be quite useless to consider equation (2) in this context. The difficulty in drawing the curve of spanwise loading in Fig. 2, especially near $\eta=0{\cdot}45$, is perhaps an indication that the validity of the standard calculation of drag from Section 2 requires to be checked. The alternative procedure in Section 3 presupposes that the spanwise loading contains logarithmically infinite slope at the inboard end of the flap. This is consistent with the principles underlying the spanwise equivalent slopes (Ref. 4, Section 4.2)

that are used in obtaining γ. Until there is a reliable linearized solution for the load distribution incorporating both chordwise and spanwise discontinuities in downwash across the perimeter of the flap, the accuracy of γ remains unconfirmed. In Section 4, therefore, a novel approach to the evaluation of vortex drag is described; by use of a reverse-flow theorem the factor K can be determined without prior knowledge of the spanwise loading.

2. *Standard Method.*

All routine calculations of vortex drag involve the assumption that the spanwise loading can be represented by a finite Fourier series such as

$$\gamma=\sum_{p=1}^{\frac{1}{2}(m+1)} A_{2p-1}\sin(2p-1)\theta \text{ with } \eta=\cos\theta\ ; \tag{5}$$

asymmetrical spanwise loading would naturally introduce additional terms $A_{2p}\sin 2p\theta$. For convenience, the upper limit to the summation, $p=\frac{1}{2}(m+1)$, is taken as the number of spanwise collocation positions on the half wing

$$\eta=\eta_n=\sin\frac{n\pi}{m+1} \text{ with } n=0, 1, \ldots . \tfrac{1}{2}(m-1)\,. \tag{6}$$

A definition of vortex drag coefficient, consistent with Ref. 2 and with Multhopp's[5] method, is

$$C_{Dv}=A\int_{-1}^{1}\gamma\,\alpha_i\,d\eta\,, \tag{7}$$

where the so-called induced incidence

$$\alpha_i=\frac{1}{2\pi}\int_{-1}^{1}\frac{d\gamma}{d\eta'}\frac{d\eta'}{\eta-\eta'}\,. \tag{8}$$

The resulting formula from equation (147) of Ref. 5 is

$$\frac{C_{Dv}}{\pi A}=\tfrac{1}{4}\gamma_0^2+\tfrac{1}{2}\sum_{\nu=1}^{\frac{1}{2}(m-1)}\gamma_\nu^2-\sum_{\substack{\nu=1\\(odd)}}^{\frac{1}{2}(m-1)}\ \sum_{\substack{n=-\frac{1}{2}(m-1)\\(even)}}^{\frac{1}{2}(m-1)} a_{\nu n}\,\gamma_\nu\,\gamma_n\,, \tag{9}$$

where the quantities γ_n, and similarly γ_ν, stand for $\gamma(\eta_n)$ at the collocation sections in equation (6), spanwise symmetry imposes $\gamma_{-n}=\gamma_n$, and for $|n-\nu|$ odd

$$a_{\nu n}=\frac{4(1-\eta_\nu^2)(1-\eta_n^2)}{(m+1)^2(\eta_\nu-\eta_n)^2}\,. \tag{10}$$

The corresponding lift coefficient is calculated as

$$C_L = \frac{2\pi A}{m+1}\left[\tfrac{1}{2}\gamma_0 + \sum_{n=1}^{\frac{1}{2}(m-1)} \gamma_n \cos\frac{n\pi}{m+1}\right]. \tag{11}$$

Equations (9) and (11) with $m=15$ have been used to calculate C_{D_v} and C_L from the values of γ_n in Table 1 obtained in Ref. 4 with the 15 collocation sections. The results in Table 2 corresponding to $m=7$ only involve the alternate values of γ from the same solution. The lift coefficient increases by 6 per cent when the number of integration points is increased, but the result $C_L=0{\cdot}751$ from equation (11) with $m=15$ is in close agreement with the lift derivative $-2z_\xi=0{\cdot}752$ from the different solution in Table 13a of Ref. 4. The drag coefficient is less sensitive, however, and only increases by $2\frac{1}{2}$ per cent when m is increased from 7 to 15 in equation (9). The vortex drag factor $K=4{\cdot}02$ is obtained, and the value is some 30 to 40 per cent greater than the corresponding results from certain unpublished theoretical data intended for data sheets. This highlights the need for the present investigation.

3. *Alternative Direct Method.*

The spanwise loading for a deflected part-span flap is thought to have a logarithmically infinite slope at the position $\eta=\eta_a$, which cannot be represented by equation (5). The distribution of γ_n in Table 1 is obtained by the method of Ref. 4, in which the implicit form of symmetrical spanwise loading is

$$\gamma = \sum_{p=1} A_{2p-1} \sin(2p-1)\theta + B_1\gamma_I + B_2\gamma_{II}, \tag{12}$$

where from equations (73) and (74) of Ref. 4 with $\eta_a=\cos\theta_a$ and with a factor of 2

$$\gamma_I = \frac{2}{\pi}\left[2\theta_a \sin\theta + (\cos\theta_a - \cos\theta)\, ln\left|\frac{\sin\frac{1}{2}(\theta-\theta_a)}{\sin\frac{1}{2}(\theta+\theta_a)}\right| + \right.$$

$$\left. + (\cos\theta_a + \cos\theta)\, ln\left|\frac{\cos\frac{1}{2}(\theta+\theta_a)}{\cos\frac{1}{2}(\theta-\theta_a)}\right|\right] \tag{13}$$

and

$$\gamma_{II} = \frac{1}{\pi}\left[2(\sin\theta_a - 2\theta_a\cos\theta_a)\sin\theta - \right.$$

$$-(\cos\theta_a - \cos\theta)^2\, ln\left|\frac{\sin\frac{1}{2}(\theta-\theta_a)}{\sin\frac{1}{2}(\theta+\theta_a)}\right| -$$

$$\left. -(\cos\theta_a + \cos\theta)^2\, ln\left|\frac{\cos\frac{1}{2}(\theta+\theta_a)}{\cos\frac{1}{2}(\theta-\theta_a)}\right|\right]. \tag{14}$$

When equations (12) to (14) are substituted in equation (8), it can be shown that

$$\left.\begin{aligned}
\alpha_i &= \sum_{p=1} \frac{(2p-1)\,A_{2p-1}\sin(2p-1)\,\theta}{2\sin\theta} && (\theta_a<\theta<\pi-\theta_a)\\
&= \sum_{p=1} \frac{(2p-1)\,A_{2p-1}\sin(2p-1)\,\theta}{2\sin\theta} + && \\
&\quad +B_1+B_2(|\cos\theta|-\cos\theta_a) && \begin{matrix}(0<\theta<\theta_a,\\ \pi-\theta_a<\theta<\pi)\end{matrix}
\end{aligned}\right\} \qquad (15)$$

The discontinuities in α_i are basic to the alternative method. Although they imply unrealistic spanwise discontinuities in downwash in the wake, these are necessary to satisfy a true linearized solution for the part-span flap. Then by equations (7), (12) and (15)

$$\frac{C_{Dv}}{A} = \int_0^{\pi} \gamma\alpha_i \sin\theta\, d\theta$$

$$= \int_0^{\pi} \gamma \sum_{p=1} \tfrac{1}{2}(2p-1)\,A_{2p-1}\sin(2p-1)\,\theta\, d\theta +$$

$$+\left(\int_0^{\theta_a} + \int_{\pi-\theta_a}^{\pi}\right)\gamma\left\{B_1+B_2(|\cos\theta|-\cos\theta_a)\right\}\sin\theta\, d\theta$$

$$=\tfrac{1}{4}\pi \sum_{p=1} (2p-1)\,A_{2p-1}^2 +$$

$$+\tfrac{1}{2}\sum_{p=1}\int_0^{\pi}(2p-1)\,A_{2p-1}\sin(2p-1)\,\theta\left\{B_1\gamma_I+B_2\gamma_{II}\right\}d\theta +$$

$$+2\sum_{p=1}\int_0^{\theta_a} A_{2p-1}\sin(2p-1)\,\theta\left\{B_1+B_2(\cos\theta-\cos\theta_a)\right\}\sin\theta\, d\theta +$$

$$+2\int_0^{\theta_a}\left\{B_1\gamma_I+B_2\gamma_{II}\right\}\left\{B_1+B_2(\cos\theta-\cos\theta_a)\right\}\sin\theta\, d\theta\,. \qquad (16)$$

In the present application, with constant flap chord ratio E, the procedure in Ref. 4 for spanwise equivalent slopes includes γ_I but not γ_{II}; we therefore set $B_2=0$ and an upper limit of summation $p=\frac{1}{2}(m-1)$ to give $\frac{1}{2}(m+1)$ coefficients in equation (12). Then, after some manipulation, equation (16) yields

$$\frac{C_{Dv}}{A}=\tfrac{1}{4}\pi\sum_{p=1}^{\frac{1}{2}(m-1)}(2p-1)\,A_{2p-1}^2+A_1\,B_1\,(2\theta_a-\sin 2\theta_a)+$$

$$+\sum_{p=2}^{\frac{1}{2}(m-1)}A_{2p-1}\,B_1\left\{\frac{p-1}{p}\sin 2p\theta_a-2\cos\theta_a\sin(2p-1)\theta_a+\frac{p}{p-1}\sin(2p-2)\theta_a\right\}+$$

$$+\frac{4}{\pi}B_1^2\left\{\theta_a^2-\theta_a\sin 2\theta_a-2\cos^2\theta_a\,ln\,|\cos\theta_a|\right\}. \tag{17}$$

The corresponding formula for lift coefficient is

$$\frac{C_L}{A}=\int_0^{\pi}\gamma\sin\theta\,d\theta$$

$$=\tfrac{1}{2}\pi A_1+B_1(2\theta_a-\sin 2\theta_a). \tag{18}$$

It remains to determine the coefficients A_{2p-1} and B_1 so that equation (12) satisfies the $\frac{1}{2}(m+1)$ values of γ_n in Table 1, to substitute the values in equations (17) and (18), and finally to evaluate K from equation (1).

The calculations are made for $m=15$ and as if $m=7$. The linear simultaneous equations give the following solutions.

m	A_1	A_3	A_5	A_7	A_9	A_{11}	A_{13}	B_1
7	−0·4025	−0·0439	0·0309	—	—	—	—	0·5870
15	−0·3065	−0·0154	0·0263	−0·0037	−0·0001	0·0015	−0·0013	0·4777

The extra coefficients in the case $m=15$ are commendably small. Table 2 shows that the lift coefficients in the two cases are much closer than those from equation (11) used in the standard method of Section 2; likewise the vortex drag factors are much closer. The value $K=3{\cdot}92$ with $m=15$ is only $2\frac{1}{2}$ per cent below the result from Section 2; incidentally, the difference arises from individual discrepancies in C_L and C_{Dv} of less than 1 per cent.

4. *Use of Reverse-Flow Theorem.*

The comparisons between the direct methods of Sections 2 and 3 suggest that, given the spanwise loading, there are adequate numerical techniques for obtaining the vortex drag factor. There remains, however, an element of uncertainty regarding the spanwise loading itself. In the absence of a definitive solution to the linearized problem, without the use of equivalent slopes, a suspicion of inaccuracy will remain.

Let us suppose that the spanwise loading in equation (5) is replaced by the infinite Fourier series

$$\gamma=\sum_{p=1}^{\infty} A_{2p-1}\sin(2p-1)\theta\,. \tag{19}$$

Then, by equations (17) and (18) with $B_1=0$, we have

$$K=\frac{\pi A C_{Dv}}{C_L^2}=\sum_{p=1}^{\infty}(2p-1)\left(\frac{A_{2p-1}}{A_1}\right)^2. \tag{20}$$

Although equation (19) is expected to be a slowly convergent series, that for vortex drag, involving the squares of the coefficients, should converge relatively quickly. It follows from equation (19) that

$$A_{2p-1}=\frac{2}{\pi}\int_0^{\pi}\gamma\sin(2p-1)\theta\,d\theta\,. \tag{21}$$

Consistent with equation (4), the non-dimensional circulation can be written as

$$\gamma=\frac{1}{4s}\int l\,dx\,, \tag{22}$$

where l is the local wing loading as a fraction of the stream dynamic pressure and the integral is taken from leading to trailing edge at the section $y=s\cos\theta$. By equations (21) and (22), A_{2p-1} can be expressed as a generalized force coefficient

$$A_{2p-1}=\frac{1}{2\pi s^2}\iint_S l\,\overline{W}_{2p-1}\,dx\,dy\,, \tag{23}$$

where S denotes the area of planform and the force mode

$$\overline{W}_{2p-1}=\frac{\sin(2p-1)\theta}{\sin\theta}. \tag{24}$$

Now we can invoke the general reverse-flow theorem due to Flax[6] (1952), to transform the double integral (23) so that

$$A_{2p-1}=\frac{1}{2\pi s^2}\iint_S \bar{l}_{2p-1}\,W\,dx\,dy\,, \tag{25}$$

where $\bar{l}_{2p-1}$ is the non-dimensional loading on the wing with reversed stream and the downwash mode or twist distribution from equation (24), and the force mode W corresponds to the downwash angle associated with the loading l, namely

$$\left.\begin{aligned} &W=1 \text{ on the flaps}\\ &W=0 \text{ off the flaps}\end{aligned}\right\}. \tag{26}$$

For the untapered wing, equation (25) reduces to

$$A_{2p-1}=\frac{1}{\pi A}\int\int \bar{l}_{2p-1}\, d(x/c)\, d\eta\,, \tag{27}$$

where the integral is taken over the area of the two flaps.

Although the region of integration includes typical leading-edge singularities in $\bar{l}_{2p-1}$, this loading on the reversed (swept-forward) wing corresponds to the smooth downwash mode of equation (24). Reliable solutions for $\bar{l}_{2p-1}$ can therefore be obtained, provided that p is not too large in relation to the number of spanwise collocation points. The loadings are calculated from a version of the lifting-surface theory of Zandbergen et al[7] (1967), re-programmed by Mr. P. S. Hampton of the Division of Numerical and Applied Mathematics, N.P.L. As there are 4 chordwise by 23 spanwise collocation points and 95 spanwise integration points between the wing tips, the results are expected to be reasonably accurate up to about $p=8$.

The loading on the reversed wing takes the form

$$\bar{l}_{2p-1}=\frac{8s}{\pi c}\sum_{q=1}^{4}\Gamma_q(\theta)\frac{\cos(q-1)\,\phi+\cos q\phi}{\sin\phi}, \tag{28}$$

where in terms of the leading edge of the actual wing

$$x-x_l=\tfrac{1}{2}c(1+\cos\phi)\,. \tag{29}$$

The flaps correspond to regions $(0<\theta<\theta_a, 0<\phi<\phi_h)$ and $(\pi-\theta_a<\theta<\pi, 0<\phi<\phi_h)$, where

$$\cos\phi_h=1-2E\,. \tag{30}$$

By equations (27) to (30) and by spanwise symmetry

$$A_{2p-1}=\frac{4}{\pi^2}\int_{\eta_a}^{1}\int_{0}^{\phi_h}\sum_{q=1}^{4}\Gamma_q(\theta)\{\cos(q-1)\,\phi+\cos q\phi\}\,d\phi\,d\eta$$

$$=\frac{4}{\pi^2}\int_{0}^{\theta_a}\Big[\Gamma_1(\theta)(\phi_h+\sin\phi_h)+\Gamma_2(\theta)(\sin\phi_h+\tfrac{1}{2}\sin 2\phi_h)+$$

$$+\Gamma_3(\theta)(\tfrac{1}{2}\sin 2\phi_h+\tfrac{1}{3}\sin 3\phi_h)+$$

$$+\Gamma_4(\theta)(\tfrac{1}{3}\sin 3\phi_h+\tfrac{1}{4}\sin 4\phi_h)\Big]\sin\theta\,d\theta\,. \tag{31}$$

The integrand is readily evaluated when $E=0{\cdot}25$, and numerical spanwise integration for each p with $\theta_a=\cos^{-1}(0{\cdot}45)$ gives the coefficients A_{2p-1} in Table 3. The final step is to calculate K from equation (20) with a variable upper limit of summation $p=\frac{1}{2}(m+1)=1, 2, \ldots. 8$. The results in Table 3 show a useful

degree of convergence; two terms are insufficient and give no better accuracy than would equation (2), nor are four terms quite enough as is shown by the value $K=3{\cdot}84$ included under $m=7$ in Table 2. When all 8 coefficients are used, there is the final value $K=3{\cdot}97$, which lies midway between the values for $m=15$ from the preceding direct methods. The discrepancies are less than $\pm 1\frac{1}{2}$ per cent, and it is reasonable to conclude that the present calculation of vortex drag approximates to the true linearized result to this order of accuracy.

5. *Discussion.*

It is possible to discuss the nature of the errors in approximating to equation (20). Since every term is positive, truncation of the series with exact values of A_{2p-1} would clearly lead to an underestimate of K. On the other hand, collocation with any fixed number of spanwise stations (23 in the present application) would inevitably introduce errors, and eventually random divergence, in A_{2p-1} if $(2p-1)$ were to approach and then exceed that number; such a calculation would lead to an overestimate of K. In the present calculation with $2p-1 \leqslant 15$, the two types of error are thought to be reasonably small and of the same order of magnitude.

The reverse-flow theorem is such that, having made calculations for a particular flap, we can use the same sets of coefficients $\Gamma_q(\theta)$ at the collocation sections to evaluate K for any other size of flap; for the given planform, the modes $\overline{W}_{2p-1}$ and loadings $\bar{l}_{2p-1}$ in equations (24) and (28) are independent of flap geometry. A simple change of flap span only affects the range of integration in equation (31),

$$\left.\begin{array}{ll} 0<\theta<\theta_a=\cos^{-1}\eta_a & \text{for outboard flaps} \\ \cos^{-1}\eta_f=\theta_f<\theta<\frac{1}{2}\pi & \text{for inboard flaps} \end{array}\right\}. \tag{32}$$

The calculation

$$K=\sum_{p=1}^{\frac{1}{2}(m+1)}(2p-1)\left(\frac{A_{2p-1}}{A_1}\right)^2 \tag{33}$$

with $m=15$ has been made for fixed chord ratio $E=0{\cdot}25$ with variable η_a or η_f, and Fig. 3 illustrates the sensitivity of the vortex drag factor to flap span.

An infinite limit is expected as $\eta_a \to 1$ or $\eta_f \to 0$. It is worth noting that, if B_1 were the dominant coefficient in equation (12) as $\eta_a \to 1$, then equations (17) and (18) would give $K=0(1-\eta_a)^{-1}$. To simulate the limit $\eta_f \to 0$, we might set $A_1=-2B_1$ as dominant coefficients in equation (12) and deduce similarly that $K=0(\log \eta_f{}^{-1})$. These limiting forms would apply to a slender planform with unswept trailing edges (Ref. 8); they also provide some qualitative explanation of the behaviour of the respective curves of K in Fig. 3.

To study the effect of flap chord, the spanwise integrals in equation (31) are evaluated before the numerical values of ϕ_h are substituted. For fixed $\eta_a=0{\cdot}45$, the vortex drag factor has been evaluated for the full range of E, $0<\phi_h<\pi$ in equation (30). Fig. 4 shows that, although there is less variation in K with flap chord than with flap span, its dependence on E is far from negligible. In preparing data sheets on the theoretical vortex drag of wing-flap combinations, flap chord ratio is a necessary parameter with more influence than one might have expected.

6. *Conclusions.*

(1) Two direct methods of calculating vortex drag from a prescribed spanwise loading and a novel third method, on the reverse-flow principle without a definitive spanwise loading, are applied to an untapered swept wing with symmetrically deflected outboard flaps. The results are consistent within $\pm 1\frac{1}{2}$ per cent.

(2) The calculations provide a reliable check point for the purpose of data sheets on the theoretical vortex drag of wing-flap combinations. No better accuracy is required or is likely to be obtainable in the present state of linearized theory.

(3) The third method (Section 4) is rather cumbersome to apply to flaps of fixed geometry, but it is well suited for studying the influence of flap span and chord (Section 5). The vortex drag factor is shown to be highly dependent on flap span and to vary significantly with flap chord ratio.

Acknowledgement.

The author acknowledges the assistance of Mrs. Sylvia Lucas of the Aerodynamics Division, N.P.L., who was responsible for carrying out and checking the calculations.

LIST OF SYMBOLS

a_{vn}	Coefficient in equation (10)
A	Aspect ratio of wing
A_{2p-1}	Coefficient in equation (5), (12) or (27)
B_1, B_2	Coefficients in equation (12)
c	Chord of wing
C_{Dv}	Vortex drag referred to stream dynamic pressure and planform area
C_L	Lift referred to stream dynamic pressure and planform area
C_{LL}	Local lift referred to stream dynamic pressure and wing chord
E	Ratio of flap chord to wing chord
K	Vortex drag factor in equation (1)
l	Local wing loading referred to stream dynamic pressure
l_{2p-1}	Non-dimensional loading on reversed wing corresponding to $\overline{W}_{2p-1}$
m	Parameter controlling the number of terms in equation (9), (17) or (33)
n	Integer or subscript to denote a collocation position
p	Integer to denote a coefficient A_{2p-1}
q	Integer to denote chordwise loading in equation (28)
s	Semi-span of wing
S	Area of planform
W	Discontinuous force or downwash mode in equation (26)
$\overline{W}_{2p-1}$	Smooth force mode or twist distribution in equation (24)
x	Streamwise distance
x_l	Local ordinate of leading edge
y	Spanwise distance from centre line of wing
α_i	Induced incidence in equation (8)
γ	Non-dimensional circulation in equation (4) or (22)

γ_I, γ_{II}	Spanwise loadings in equations (13), (14)
γ_n, γ_ν	Values of γ at collocation positions $\eta = \eta_n, \eta_\nu$
Γ_q	Coefficient in equation (28)
η	Non-dimensional spanwise distance y/s
$\bar{\eta}$	Spanwise centre of pressure in equation (3)
η_a	Value of $\lvert\eta\rvert$ at inboard end of outboard flap
η_f	Value of $\lvert\eta\rvert$ at outboard end of inboard flap
η_n, η_ν	Collocation positions in equation (6) or similar one in ν
θ	Angular spanwise parameter $\cos^{-1}\eta$
θ_a, θ_f	Values of θ corresponding to $\eta = \eta_a, \eta_f$ in equation (32)
Λ	Angle of sweepback
ν	Subscript to denote a collocation position
ϕ	Angular chordwise parameter in equation (29)
ϕ_h	Location of flap hinge on reversed wing in equation (30)

REFERENCES

No.	*Author(s)*	*Title, etc.*
1	Royal Aeronautical Society ..	Subsonic lift-dependent drag due to wing trailing vortices. Aerodynamics Data Sheet WINGS 02.01.02. October, 1965.
2	H. C. Garner	Some remarks on vortex drag and its spanwise distribution in incompressible flow. *Aeronaut. J. (R.Ae.S.) Vol. 72,* pp. 623-625. July, 1968.
3	H. C. Garner and Sandra M. Inch	Subsonic theoretical lift-curve slope, aerodynamic centre and spanwise loading for arbitrary aspect ratio, taper ratio and sweepback. A.R.C., C.P. 1137. May, 1970.
4	H. C. Garner and Doris E. Lehrian	The theoretical treatment of slowly oscillating part-span control surfaces in subsonic flow. A.R.C., R. & M. 3676. October, 1969.
5	H. Multhopp	Methods for calculating the lift distribution of wings (Subsonic lifting surface theory). A.R.C., R. & M. 2884. January, 1950.
6	A. H. Flax	General reverse-flow and variational theorems in lifting-surface theory. *J. Aero. Sci., Vol. 19,* pp. 361-374. June, 1952.
7	P. J. Zandbergen, Th. E. Labrujere and J. G. Wouters	A new approach to the numerical solution of the equation of subsonic lifting surface theory. N.L.R. Report TR G.49. November, 1967.
8	J. De Young	Spanwise loading for wings and control surfaces of low aspect ratio. N.A.C.A. Technical Note 2011. January, 1950.

TABLE 1

Spanwise Loading on an Untapered Wing ($A=4$, $\Lambda=45°$) with Outboard Flaps ($E=0{\cdot}25$, $\eta_a=0{\cdot}45$) at Symmetrical Unit Deflection.

n		η_n	γ_n
$m=7$	$m=15$		
0	0	0	0·0143
	1	0·1951	0·0187
1	2	0·3863	0·0427
	3	0·5556	0·1467
2	4	0·7071	0·1770
	5	0·8315	0·1728
3	6	0·9239	0·1419
	7	0·9808	0·0805

TABLE 2

Calculated Lift and Vortex Drag by Various Methods.

Method	$m=7$			$m=15$		
	C_L	C_{Dv}	K	C_L	C_{Dv}	K
Section 2	0·710	0·1760	4·38	0·751	0·1804	4·02
Section 3	0·768	0·1892	4·03	0·758	0·1791	3·92
Section 4	0·749	0·1714	3·84	0·749	0·1774	3·97

TABLE 3

Coefficients and Vortex Drag Factor from Reverse Flow.

p or $\frac{1}{2}(m+1)$	1	2	3	4	5	6	7	8
A_{2p-1}	0·1192	0·1150	−0·0095	−0·0051	0·0114	−0·0066	−0·0004	0·0041
K	1·000	3·794	3·826	3·839	3·921	3·955	3·955	3·973

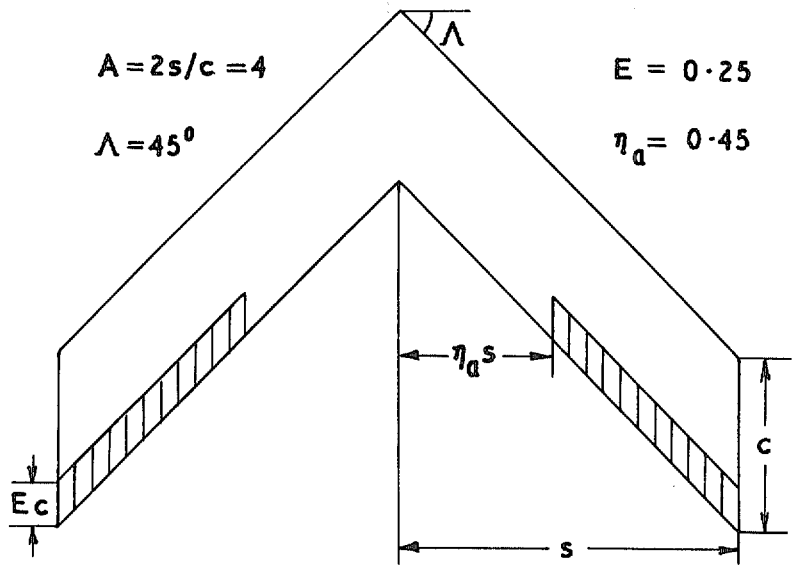

FIG. 1. Planform geometry of wing and flaps.

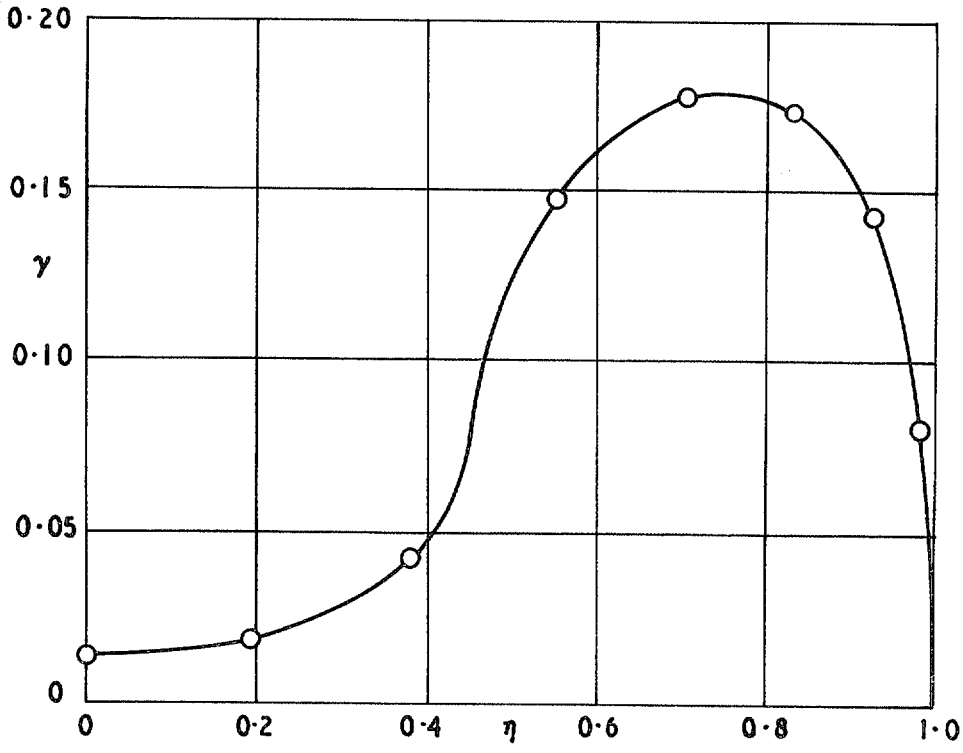

FIG. 2. Symmetrical spanwise loading with flaps at unit deflection.

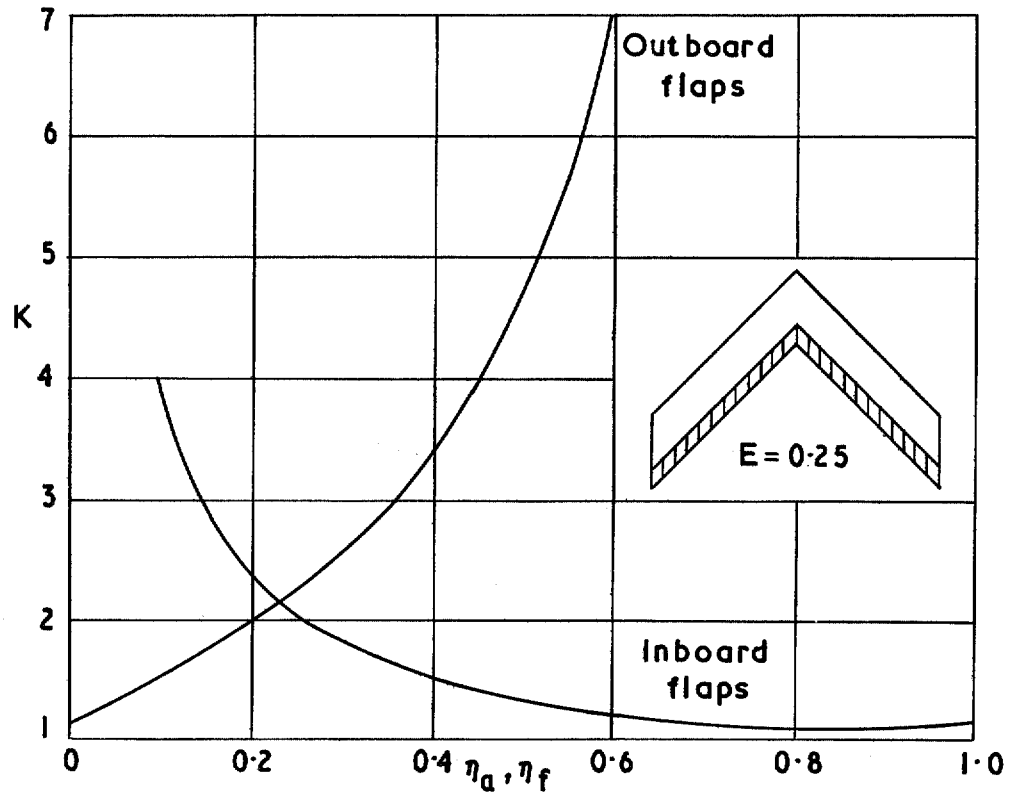

FIG. 3. Effects of flap span on vortex drag factor.

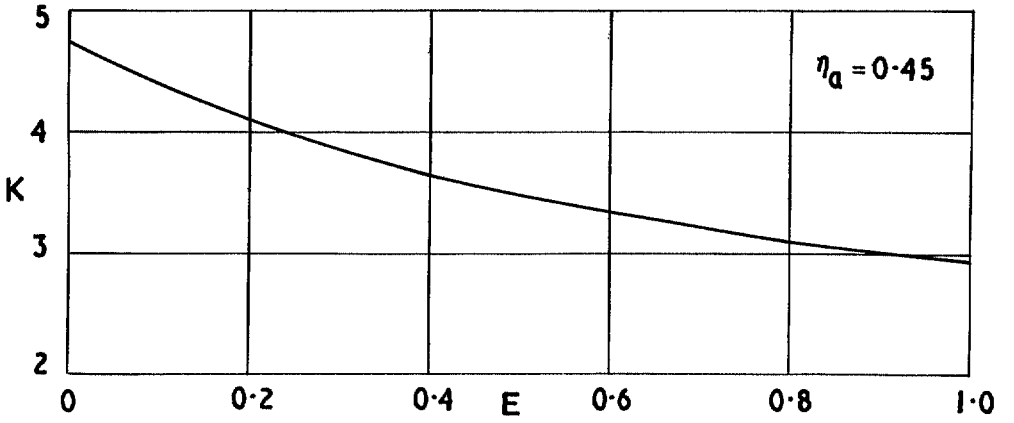

FIG. 4. Effect of flap chord on vortex drag factor.

Printed in Wales for Her Majesty's Stationery Office by Allens Printers (Wales) Limited

Dd. 502110 K.5. 4/72.

HER MAJESTY'S STATIONERY OFFICE

Government Bookshops

49 High Holborn, London WC1V 6HB
13a Castle Street, Edinburgh EH2 3AR
109 St Mary Street, Cardiff CF1 1JW
Brazennose Street, Manchester M60 8AS
50 Fairfax Street, Bristol BS1 3DE
258 Broad Street, Birmingham B1 2HE
80 Chichester Street, Belfast BT1 4JY

Government publications are also available through booksellers

SBN 11 470495 3